Tellus (2008)
Printed in Singapore. All rights reserved

TELLUS

Clustering of cyclones in the ARPEGE general circulation model

By NILS GUNNAR KVAMSTØ[1,2]*, YONGJIA SONG[2], IVAR AMBJØRN SEIERSTAD[1], ASGEIR SORTEBERG[2] and DAVID. B. STEPHENSON[1,3], [1]*Geophysical Institute, University of Bergen, Allegaten 70, N-5007, Norway;* [2]*Bjerknes Centre for Climate Reasearch, University of Bergen, Allegaten 70, N-5007, Norway;* [3]*School of Engineering, Computer Science and Mathematics, University of Exeter, Harrison Building Room 334, North Park Road, Exeter EX4 4QF, UK*

(Manuscript received 30 March 2007; in final form 27 December 2007)

ABSTRACT

Baroclinic waves give major contributions to the climatology and variability of key climate variables in mid- and high-latitudes. An important aspect of cyclone variability is the seriality (succession of cyclone occurrence). Serial cyclones are clustered in time and are associated with large economic losses in Europe. Cyclone variability and seriality are intimately linked to the low frequency variability. To have a realistic representation of high and mid-latitude regional climate in general circulation models (GCM), it is of vital importance that the described phenomena are realistically represented. In the present paper we evaluate the ability of the atmospheric GCM ARPEGE to represent various storm track parameters, both with respect to climatology and variability. Cyclone tracks are identified for the Northern Hemisphere during 55 extended winters (1950/51–2004/05) using the NCEP reanalyses by means of an objective tracking method. A corresponding cyclone track data set is derived from a simulation with ARPEGE, forced with observed monthly SSTs from 1950 to 2004. The comparison of the two data sets shows that ARPEGE reproduces the main features of the observed cyclone track fields. The mid-latitude corridors of cyclones and cyclone variability are well reproduced. The model, however, underestimates the mean number of cyclone occurrence and its variance. In the eastern North Atlantic and Nordic Seas the model simulates 70 and 90% of the observed mean cyclone occurrence and its variance, respectively. ARPEGE also substantially underestimates the clustering of cyclones in the eastern North Atlantic (jet exit region). In addition, the model also fails to simulate the relationship between clustering and low-frequency flow patterns at the exit of the North Atlantic storm track.

1. Introduction

The mid-latitude storm-track plays a key role in determining the climatology in the extratropics and high latitudes. This is mainly because baroclinic waves constitute a main agent for transporting heat, moisture and momentum polewards (Peixoto and Oort, 1992; Hartmann, 1994). In the North Atlantic region baroclinic waves are particularly important since we here find one of the highest occurrences of synoptic lows in the Northern Hemisphere. Since the Bergen School developed the cyclone model (Bjerknes, 1910), air-flows associated with extratropical cyclones have been extensively studied. Our present conceptual understanding of the cyclone is based on a quasi-Lagrangian conveyor belt model developed by Harrold (1973), Browning et al. (1973) and Carlson (1980). In this model we find three airstreams in a coordinate system following the surface low. These airstreams are named the dry intrusion, the cold conveyorbelt and the warm conveyorbelt (for details see Browning, 1990, 1999; Carlson, 1998). Most of the heat transport (both latent and sensible) associated with cyclones, takes place in the warm conveyorbelt (WCB). The WCB originates in the atmospheric boundary layer in the cyclone's warm sector and the air parcels ascend slantwise ahead of the surface cold front all the way into the upper troposphere. The depth and width are typically 1 km and a few hundred km, respectively. Massive cloud formation, latent heat release and precipitation are associated with the WCB. In a comprehensive description of the global WCB climatology by Eckhardt et al. (2004), it is shown that up to 72% of the winter precipitation in the North Eastern North Atlantic, Northern Europe and Nordic Seas is tied to the WCB. During winter on the Northern Hemisphere, Eckhardt et al. (2004) found a close correspondence between the number of lows and the number of WCBs. Thus nearly all lows in the North Atlantic are associated with a WCB during winter.

*Corresponding author.
e-mail: Nils.Kvamsto@gfi.uib.no
DOI: 10.1111/j.1600-0870.2008.00307.x

Cyclone occurrence and cyclone strength in the North Atlantic during winter exhibit high variability on scales ranging from decades to synoptic time scales (Sorteberg et al., 2004). On interannual and larger scales, the North Atlantic storm track variability is linked to the large scale circulation, mainly represented by the North Atlantic Oscillation (NAO) (Hurrell, 1995) or Arctic Oscillation AO (Thompson and Wallace, 1998). During winters with high NAO/AO index (stronger westerlies than normal) we find an intensification, an increased occurrence and a northward shift of the North Atlantic storm track (Rogers 1997; Sorteberg et al. 2004). The Eastern part of the storm track is also directed more cross latitudinally towards the north in the positive phase. During the negative phase the North Atlantic storm track shifts southward, is less intense and is directed more zonally. It should also be mentioned that the correlation between storm track parameters and the NAO/AO in the North Atlantic changes with time over the data record 1950–2000 (Raible et al., 2001; Sorteberg et al., 2004; Luksch et al., 2005).

This linkage between storm track variability and the NAO/AO index concerns only integrated storm track parameters. Mailier et al. (2006) (hereafter denoted as M06) analysed individual cyclone trajectories during winter in the period 1950–2003. Application of a Poisson regression showed that the variation of monthly cyclone occurrences over northeastern North Atlantic, the Nordic Seas and Europe is largely accounted for by modes of climate variability with lower frequency than the synoptic scale. One should note that several other patterns in addition to the NAO/AO play a crucial role here. A closer investigation of the time-behaviour of cyclones shows that there are regions with more serial clustering of lows than expected due to chance (overdispersion). M06 also found regions of underdispersion, or higher regularity of lows than expected due to chance, in addition to areas with more random behaviour. Implicitly, the seriality is also accounted for by the lower frequency patterns since the dispersion statistic is a function of variability. It is relevant to note that serial storms which cluster in time represent a cyclone class that can have a devastating effect on European economy (M06).

In summary the listed work demonstrates the crucial impact of baroclinic waves on the regional climatology, variability and distribution of extreme events (and thereby a number of important impact parameters as well) and their intimate link to the large scale flow. Under such circumstances a GCM ought to have a realistic representation of the storm track and the lower frequency patterns in order to obtain as much added value as possible from a subsequent regional dynamic downscaling.

In this paper, we explore how the ARPEGE GCM (Déqué et al., 1994) simulates the mid-latitude storm track, with particular emphasis on Northern Europe, North Eastern North Atlantic and the Nordic Seas. Northern Hemisphere cyclone tracks during 55 extended winters (1950/51–2004/2005) has been identified in NCEP reanalyses by means of an objective tracking method (Hodges, 1995; 1996). Corresponding cyclone track data sets are identified from a hindcast simulation with ARPEGE, forced with observed monthly SSTs from 1950 to 2004. The cyclone climatology (mean number of occurrence), variance and seriality, in particular, at grid point level are inter-compared between the two data sets. Furthermore, we investigate to what extent systematic model errors originate from deficiencies in the climatology and/or low frequency patterns.

The intercomparison of cyclone statistics between the two data sets will not be done on the basis of all cyclone trajectories. The intercomparison will be based on a subset that consists of cyclone trajectories that have their ending points located north of their starting points. The reasons for concentrating on northward moving cyclones are twofold. One is that nearly 80% of the observed cyclone trajectories move in the northward direction and it is a well-known fact that most General Circulation Models (GCM) in general (and ARPEGE in particular) have a storm track climatology which shows a too zonal North Atlantic storm track in the exit region (Doblas-Reyes et al., 1998; Lopez et al., 2000). It is thus of particular scientific interest to describe and understand differences in characteristics of northward moving cyclones between observations and GCM data. Secondly, it is the northward moving cyclones that are associated with the most intense and largest fraction of the poleward eddy heat transport (Eckhardt et al., 2004). A deeper understanding of these is thus of vital importance for assessing climate and climate change in our region of interest.

The paper is arranged as follows. In Section 2, we present the data, model and methods. Results from intercomparison of model- and observationally based cyclone statistics are listed in Section 3, while a summary and conclusions are presented in Section 4.

2. Data, model and methods

2.1. Data

In order to compute cyclone tracks, we use 6-hourly reanalyses during 55 extended winters, October to March 1950/51–2004/05, from the National Centers for Environmental Prediction/National Center for Atmospheric Research (NCEP/NCAR) (Kalnay et al., 1996; Kistler et al., 2001). Extended winters (ONDJFM) are preferred to the more conventional DJF season in order to include also autumn and spring cyclones.

Zonal and meridional wind components at 850 hPa in the Northern Hemisphere are used to compute the relative vorticity, ξ_{850}, at this level. An advantage with ξ_{850} is that this field has little influence from the background state and highlights thus small scale features. Also cyclones can be earlier detected using ξ_{850} instead of the sea level pressure. One should note that there is little difference between lower tropospheric cyclone track statistics based on NCEP/NCAR reanalyses and reanalyses from the European Centre for Medium-range Weather Forecasts (ECMWF) ERA-15 (Hodges et al., 2003; Raible et al., 2007).

2.2. Cyclone track algorithm

The ξ_{850} field can be very noisy with frontal systems beginning to be resolved; the processing is therefore performed at a spectral resolution of T42. The reduction in resolution associated with the T42 truncation provides some smoothing of the higher frequencies. In addition planetary scales for total wave numbers $n \leq 7$ are removed from the field using a filtering method discussed by Anderson et al. (2003). This spectral cut off does not make any significant change to the results since the planetary scales are relatively weak in the vorticity fields relative to the anomalies. The retained fields are searched for local extremes, which are centres for negative and positive vorticity anomalies. In this study we have concentrated on positive vorticity anomalies (cyclones), the feature points associated with low-pressure systems. Local positive relative vorticity extremes with values greater than 1×10^{-5} s^{-1} are identified and these extremes for two consecutive time steps are linked together using the image processing technique of Salari and Sethi (1990) that is based on a cost-function which evaluates track smoothness in terms of changes in direction and speed (Hodges, 1995, 1996). The technique has been generalized to the spherical domain (Hodges, 1995), which obviates the need to use projections, which may introduce systematic biases (Zolina and Gulev, 2002). Semi-stationary storms (less than 10° total displacement) and short-lived storms (lifetime less than 2 d) are removed. For further details see also Hodges (1994) and Hodges (1999).

We here focus our attention on the cyclone track occurrence itself, but calculation of descriptive statistics is provided by the use of spherical nonparametric estimators from the ensembles of feature tracks (Hodges, 1996).

2.3. The ARPEGE GCM

The atmospheric GCM used in this study is version 3 of the ARPEGE/IFS model used operationally by Météo-France and developed jointly by Météo-France and ECMWF (Déqué et al., 1994, 1998; Doblas-Reyes et al., 1998). In the version used here, we use a radiation scheme by Morcrette (1991), convective wave drag parametrisation by Bossouet et al. (1998), snow scheme by Douville et al. (1995) and increase of orographic wave drag by Lott and Miller (1997). In our experiments we employ semi-Lagrangian time intergration and a so-called linear truncation (Hortal 1998) at wave number 63 ($T63_L$) in the horizontal. This corresponds to a latitude-by-longitude grid of approximately $2.8° \times 2.8°$. The vertical discretization (Simmons and Burridge, 1981) consists of 31 layers of which 20 are in the troposphere.

In order to explore the representation of cyclone tracks in ARPEGE, we have generated a simulation where observationally based monthly global sea surface temperature (SST) and sea ice fields from 1950 to 2004 (Reynolds and Smith, 1994) are employed as lower boundary condition. The model was integrated from January 1950 to November 2004. The SST and sea-ice fields are the only external forcings with a time development. Other external forcings are either constant (carbondioxide concentration is 353 ppm and methane concentration is 1720 ppb) or exert a climatological repeated annual cycle from present day climate (i.e. solar-, aerosol- and ozone forcing).

3. Results

3.1. Mean cyclone occurrence

Figure 1a shows the monthly mean counts ($\bar{n}$) of cyclone transits past latitudinally oriented transects for the 55 winters. The transects have a length equivalent to 10° at 50°N and are centred at each grid point. The South–North (SN) transit counts range from 0 to 6 month^{-1} with typical values in the North Pacific and North Atlantic storm tracks of 2–6 month^{-1}. Regions with values above 2 month^{-1} are used to define the storm track region. In the Pacific we find the SN maximum on the eastern side of the basin and the Atlantic maximum is found south of Greenland.

The pattern of winter mean number of southward moving (NS) cyclones (Fig. 1b) is fundamentally different from the SN case. This pattern is characterised by three maxima with peak values around 3 month^{-1}. One over central Canada and North America, a second over northern Siberia and a third over North East China. A weaker secondary maximum is located over the Mediterranean Sea. Outside these maximum areas relatively small values are found.

The distributions of simulated cyclone counts of both SN and NS travelling cyclones (Figs. 1c and d) are similar to observations. However, there are systematic errors. The number of cyclones in the model is generally too low in both major storm tracks. The Atlantic storm track is also too zonal as it does not turn to the northeast in the jet exit region. Subsequently, it also penetrates too far eastward over Europe. These modelling biases are well known and are discussed by Doblas-Reyes et al. (1998) in an Eulerian framework. Biases are also evident in the simulation of NS cyclone counts. There are clearly too few south moving cyclones over northern Russia and northern Canada. Model errors in both cyclone classes are shown in Figs. 1e and f.

3.2. Regularity and clustering

Maps of the variance s^2 of monthly transit counts are shown in Figs. 2a and b for the observed and simulated cyclones. In the North Pacific both the amplitude and position of the variance seem to be well simulated. In the North Atlantic there is a slight underestimation of the variance.

By comparing Figs. 1a and c to Figs. 2a and b it is evident that the variance is similar to the mean in the regions of the major storm tracks. Areas with higher transit counts generally have higher variance. As shown in Appendix A, the distributions of monthly transit counts and their variance would be equal if the

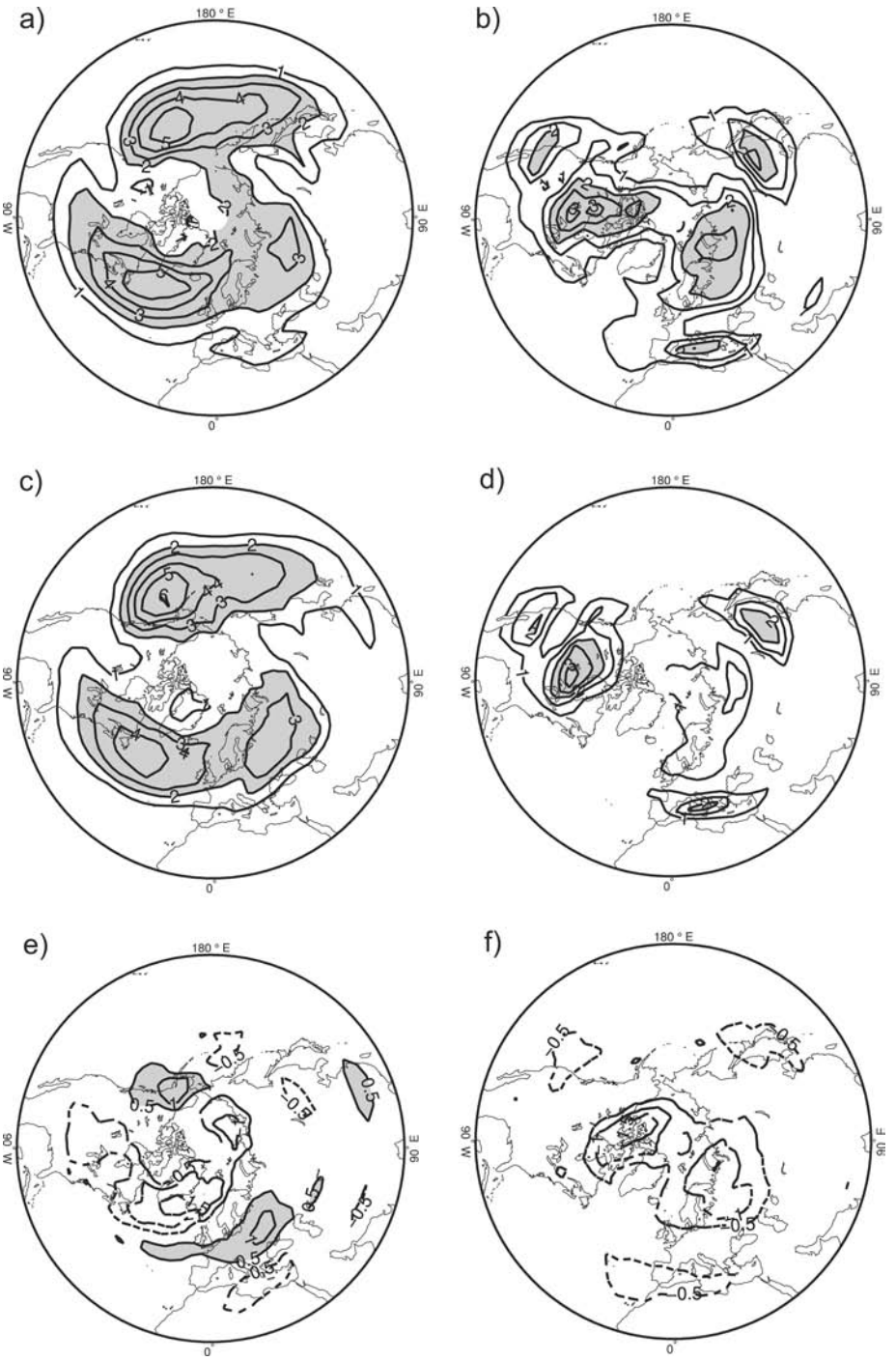

Fig. 1. Sample mean $\bar{n}$ of the monthly counts of (a) South–North directed cyclone transits based on NCEP data. The contours start at 1 month^{-1} with intervals of 1 month^{-1}. (b) North–South directed cyclone transits based on NCEP data. The contours start at 1 month^{-1} with intervals of 0.5 month^{-1}. (c) Same as (a), but for data simulated with ARPEGE. (d) Same as (b) but for data simulated with ARPEGE. (e) Difference between simulated and observationally based sample mean monthly South–North directed cyclone transits (ARPEGE–NCEP). The contour level is 0.5 month^{-1}. (f) Same as (e), but for North–South directed cyclone transits. The contour level is 0.5 month^{-1}. For clarity we use shadings for contours greater than 2 month^{-1}.

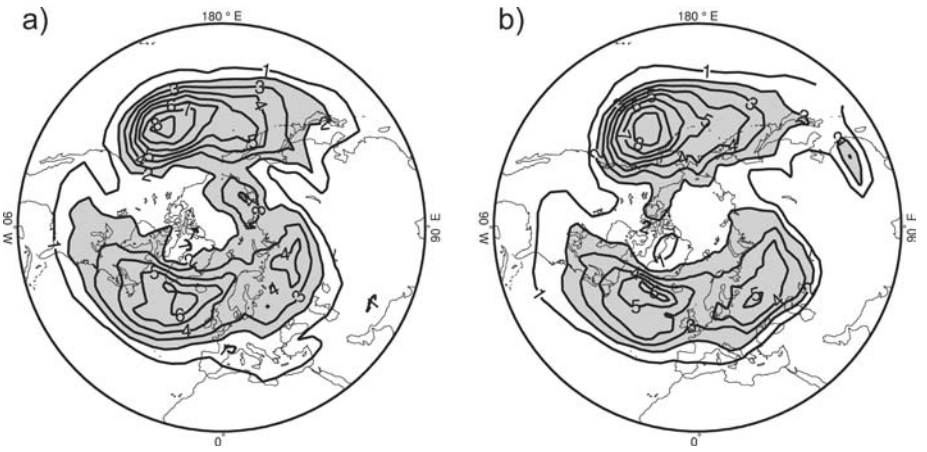

Fig. 2. Sample variance s_n^2 of the monthly number of South–North cyclone transits based on (a) NCEP data and (b) as simulated with ARPEGE. Contouring as in Fig. 1a.

cyclone counts follow a random Poisson process with constant rate.

To highlight the differences between the mean and the variance the dispersion statistic $\hat{\psi}$ is used (eq. A.1). Figure 3a shows the estimated $\hat{\psi}$ for the observed SN monthly cyclone counts. Negative values indicating underdispersion are found at the westernmost part of the two ocean basins. The cyclone counts at the entrance of the two major storm tracks are therefore more regular than those expected from a purely random process with a constant rate. The regularity of the cyclones in these areas is consistent with the strong permanent baroclinic forcing, for instance measured by the Eady growth rate at 780 hPa, found in these regions during winter (Hoskins and Valdes, 1990).

Positive values, which indicate overdispersion, are found elsewhere with maxima over the east Pacific, east North Atlantic and Europe. The cyclones therefore cluster together in areas towards the eastern end of the storm track. As such it qualitatively follows the results from M06 using WE cyclones rather than SN. The most notable difference between the two studies is over the eastern North-Atlantic where higher values are found for WE cyclones. Note also that North West Siberia, which belongs to the exit region of the North Atlantic storm track, has negative values and underdispersion in the WE case, while we find overdispersion only when considering SN transits.

In order to illustrate the difference between cyclone transits at the entrance and exit of the Atlantic storm track, the transit times of cyclones at location A (45°N, 70°W), B (50°N, 5°W) and C (65°N, 25°W) are shown in Fig. 4a for the winter 1990/1991. At location A (entrance region) the cyclone transits appear more regular than at B (exit region).

The dispersion coefficient $\hat{\psi}$ of the simulated monthly cyclone transits is shown in Fig. 3b. The overall distribution of simulated $\hat{\psi}$ shows similarity to the observed one. Overdispersion (or clustering tendency) is found in the central Pacific and the eastern North Atlantic, while in the westernmost parts of the two storm tracks we find underdispersion. The most prominent difference between the observed and simulated cyclone dispersion statistics are found in the eastern North Atlantic towards Britain and France (Fig. 3c). The cyclones in the model are considerably less clustered here than the observed ones. The model also has a large maximum over South Eastern Greenland that is not found in the observations. These model biases are illustrated in Fig. 4b where cyclone transits for the winter 1975/1976 are shown at the same locations as for the observed ones in Fig. 4a. The cyclone transits appear rather regular at both locations A (entrance region) and B (exit region). This season thus illustrates the lack of clustering in the jet exit region in the model. At location C (65°N, 25°W) the cyclones are very few and clustered during this season.

3.3. Large-scale influence

The influence of low-frequency variability on the stochastic behaviour of the synoptic lows is investigated using poisson regression. Indices of the ten leading teleconnections in the Northern Hemisphere, calculated by means of rotational principal component analysis (RPCA), were chosen as explanatory variables (representing the low frequency variability). The reader is referred to appendix B for a detailed description of the Poisson regression and the ten teleconnection indices.

Since our primary region of interest is the North Atlantic storm track, we will first focus on the influence of the North Atlantic Oscillation (NAO), which is represented by the first RPC (RPC1). The spatial NAO pattern is shown in Figs. 5a and b for the observed and simulated geopotential height at 500 hPa (Z_{500}), respectively. The simulated NAO dipole is seen to be further west compared with the observed one.

Maximum likelihood estimates of the β_k parameters for the observed NAO are shown in Fig. 6a. The influence of the NAO is clearly characterized by the dipole over the Atlantic Ocean as has been well documented in the literature (Hurrell, 1995).

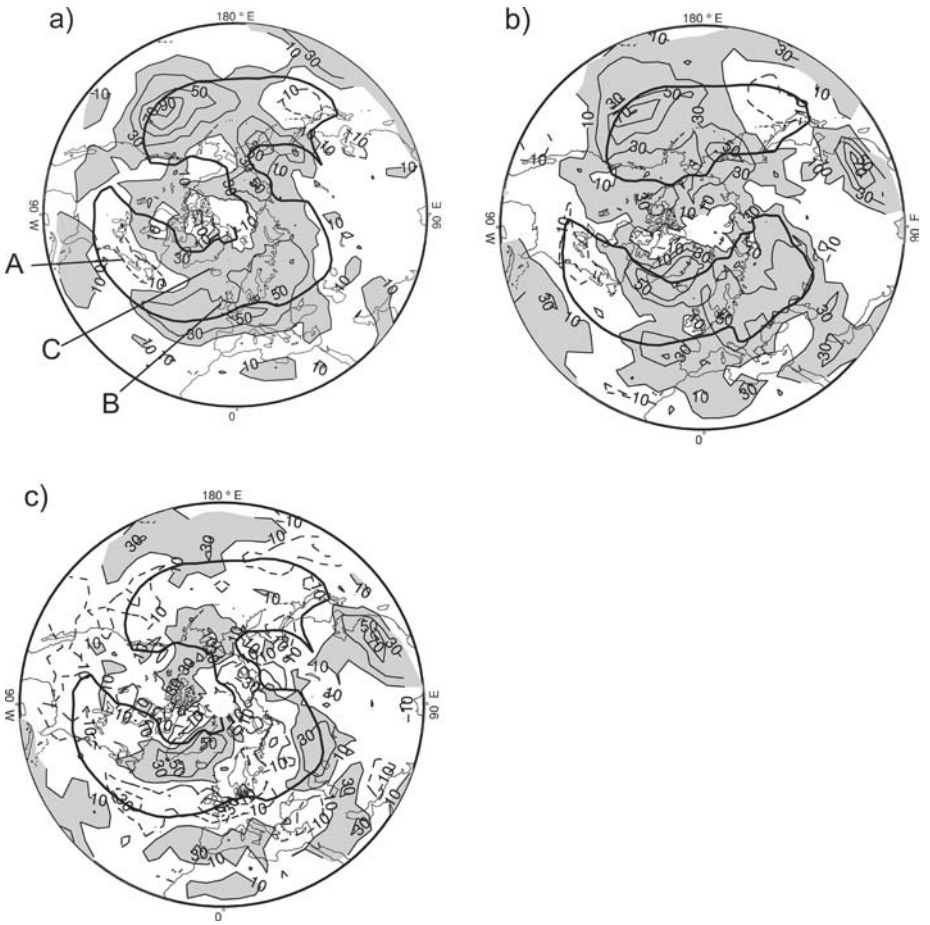

Fig. 3. (a) Estimated dispersion statistic $\hat{\psi}$ (in%) of the observed monthly number of South–North directed cyclone transits. Solid/dashed lines indicate positive/negative values. Contours start at ±10%, contour intervals at 20%. Thick lines represent the boundaries of the region where $\bar{n} \geq 2$ month^{-1}. (b) As (a), but for cyclones simulated with ARPEGE. (c) Difference between simulated and observationally based dispersion statistic $\hat{\psi}$ (in%) (ARPEGE–NCEP). Contour intervals as in (a) and (b). For clarity we use shadings for contours greater than 10%.

Its positive phase is associated with increased monthly cyclone counts in the Icelandic region and lower counts further south towards Spain and Portugal. Estimates of the β_k parameters for the simulated NAO are shown in Fig. 6b. The simulated NAO accounts for monthly cyclone transits in a very similar way to the NCEP data despite the differences in the spatial pattern.

The influence of the individual lower order teleconnection patterns in the model are also investigated (not shown). However, a visual inspection of corresponding NCEP and ARPEGE teleconnection patterns shows clearly that we do not find the same degree of correspondence for the lower order patterns as in the NAO case (not shown). Furthermore, we projected model anomalies of Z_{500} on the NCEP teleconnection patterns and applied the resulting time-series to investigate the influence of these patterns on the dispersion of the model storm tracks. The spatial teleconnection patterns would then be identical in the two data sets. Again, each of the lower order indices produced an influence pattern that corresponded poorly with its NCEP counterpart (not shown). We therefore focus on the combined influence of the ten leading teleconnection patterns. They are simply treated as a subdimensional space representing most of the low-frequency variance.

In order to investigate the combined influence of the ten teleconnection patterns on clustering a residual dispersion diagnostic is calculated. Following M06, one can estimate a dispersion coefficient that takes into account the variability of μ instead of assuming a constant μ. This is called residual dispersion and shows the remaining dispersion once the variability is accounted for by factors representing seasonality and teleconnection patterns in the Poisson regression. Plots of the estimated residual dispersion for the observed and simulated cyclone transits are shown in Figs. 7a and b, respectively. From Fig. 7a it is evident that the dispersion values are predominantly negative with the exception of a small area over France. There is no longer overdispersion at the exit of the Atlantic and Pacific storm tracks. In other words, the clustering shown in Figure 3 is largely accounted for

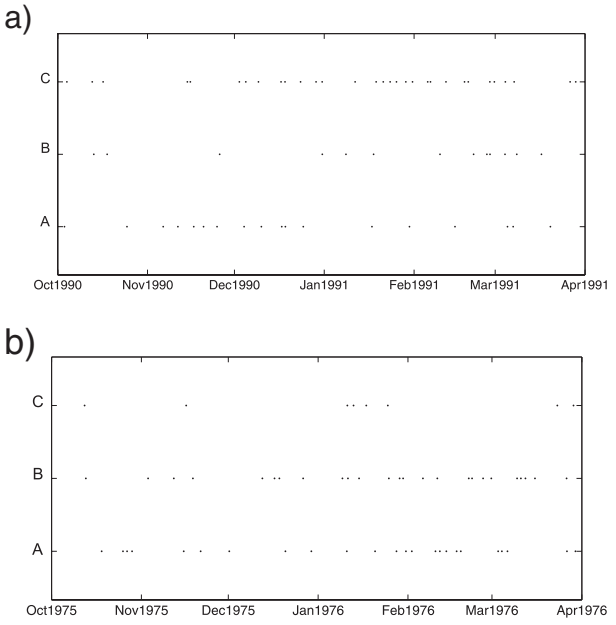

Fig. 4. (a) Point processes showing the transits of cyclones at the entrance (location A) and at the exit (locations B and C) of the North Atlantic storm track from October 1990 to April 1991. The transits are taken from the NCEP data set. (b) Same as (a), but from October 1975 to April 1976 with transits taken from the ARPEGE simulation. The specific locations are indicated by the dashed lines in Fig. 3a: A (45°N, 70°W), B (50°N, 5°W) and C (65°N, 25°W).

by the low-frequency flow patterns. This is not surprising bearing in mind the close relationship between synoptic variability and lower frequencies. Several studies have highlighted the importance of the two-way feedback between synoptic variability and the monthly mean flow (Lau, 1988; Branstator, 1995). This interaction is well known to be particularly strong in the exit regions of the storm tracks (Hoskins, 1983). The estimated residual dispersion in ARPEGE (Fig. 7b) shows that there is considerable remaining overdispersion particularly over large parts of Europe and south eastern Greenland. This suggests that there is a general model bias in representing the relationship between the clustering of cyclones and low-frequency flow patterns.

4. Summary and concluding remarks

Cyclone tracks that occurred in the Northern Hemisphere during 55 extended winters (1950/1951–2004/2005) has been identified by means of an objective tracking method (Hodges, 1995, 1996). A corresponding cyclone track data set has been derived from a simulation with the ARPEGE model, forced with observed monthly SSTs from 1950 to 2004. As we have found that the spatial structure of the monthly mean number of SN counts is similar to the corresponding WE distribution and other measures of cyclone activity (Hoskins and Hodges, 2002; Sorteberg et al., 2004; Blackmon, 1976), we have investigated SN cyclone tracks more closely. Such cyclones are most frequent and of largest importance in the North European region. Virtually all mid/high-latitude cyclone trajectories have an eastward component. As our study deals with northward moving cyclones, comparison with M06 offers the possibility to decompose structures and attribute them to either of the cyclone classes. In assessing SN cyclone counts, the most characteristic features based on NCEP data are: (i) there is positive correlation between mean number of SN cyclone counts and their monthly variability. (ii) We find clustering (overdispersion) of SN cyclone transits in the northern East Atlantic and central Pacific, while there are more regular transits (underdispersion) in the westernmost parts of the two ocean basins.

These characteristics are found to a large extent in the simulation with ARPEGE as well. However, one important exception is that the number of cyclones and its variance are systematically lower in the model data. In our region of interest, the eastern North Atlantic, Europe and Nordic Seas, the winter mean cyclone counts in the model amounts to 70% of the counts in

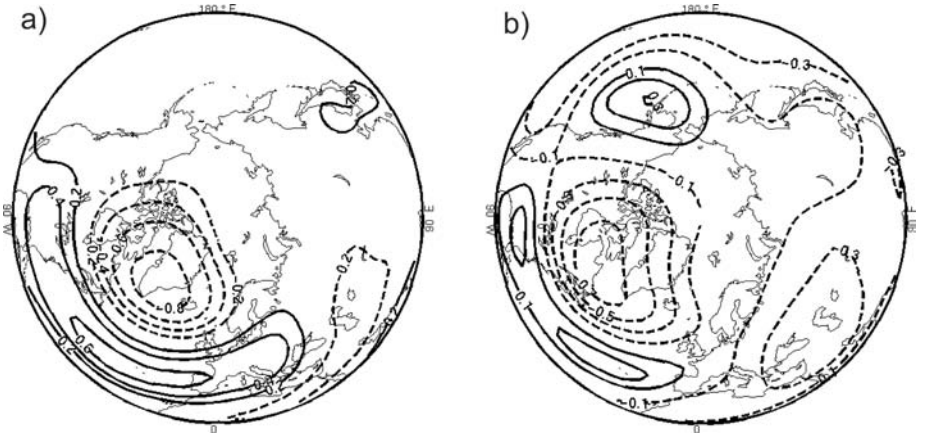

Fig. 5. (a) The spatial pattern of the NAO based on NCEP data and (b) as simulated by ARPEGE. The patterns appear as correlation coefficients (at each grid point) between the first rotated principal component (RPC1) and monthly geopotential height anomalies at 500 hPa

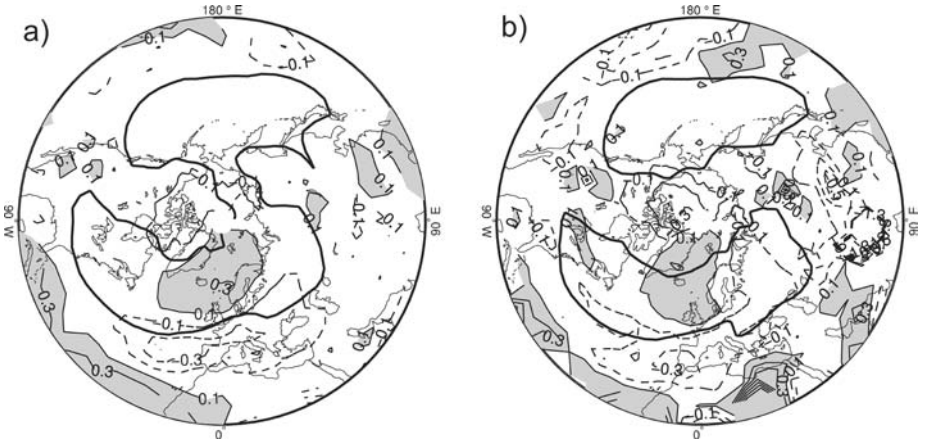

Fig. 6. (a) Estimates of the β_k parameters associated with the North Atlantic Oscillation for the South–North moving cyclones based on NCEP data. (b) Same as (a), but based on data simulated by ARPEGE. Solid/dashed lines indicate positive/negative values. Contours start at ± 0.1, contour intervals of 0.2. Areas where $\beta_k \geq 0.1$ are shaded. The estimates are based on NCEP data. For clarity we use shadings for contours greater than 0.1.

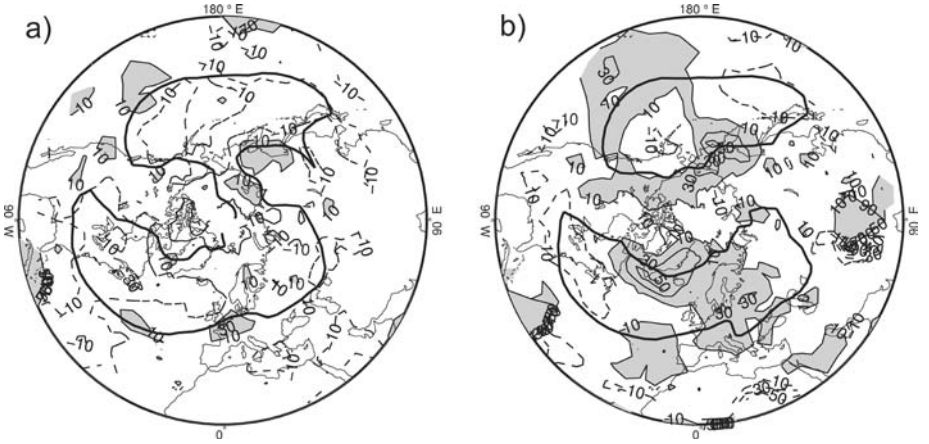

Fig. 7. The estimated residual dispersion of the monthly number of cyclone transits. Contouring is the same as in Fig. 3. For clarity we use shadings for contours greater than 10%.

NCEP for the SN cyclone class. The number for the variance of monthly counts is on average 90% of its NCEP counterpart. In addition we also find a simulated overdispersion maximum over South Eastern Greenland, which not has its counterpart in the NCEP based data set. This model bias is associated with relatively few cyclones. The most severe model deficiency is the lack of clustering of SN cyclone counts in the eastern North Atlantic.

The systematic model errors identified here have several implications apart from identifying the causalities that lead to their existence. A relevant practical problem in a 'regional climate change perspective', is that regional climate models (RCMs) are forced on the lateral boundaries with GCM fields that have deficiencies. It is an open question how these deficiencies are manifested in dynamically downscaled climate data. As the cyclone variability and seriality are intimately linked with the lower frequencies it is not likely that the improved numerical resolution and more realistic orographic forcing in a RCM completely remove the imposed errors since such models can not feed back on the larger scales. On the other hand the effect of added value from RCMs can be sensitive to the size and position of its domain. An improved understanding of these questions is vital in order to obtain better estimates of uncertainty when estimating regional climate change with RCMs. This is indeed a challenge for the modelling communities.

5. Acknowledgment

The authors want to express thanks to Dr Pascal Mailier at Reading University for helpful discussions, particularly on methodological issues. We would also like to thank Dr. Shujie Ma for providing data from the ARPEGE simulation and for helpful comments. This work has been done with support from the RegClim project (http://regclim.met.no/) funded by the Research Council of Norway. It has also received support from the Norwegian super computing Committee (TRU) through a grant of computing time on an IBM Regatta computer at Parallab, Uni-

versity of Bergen. The NCEP/NCAR data are freely downloaded from the NOAA-CIRES Climate Data Center, Boulder, Colorado, USA (http://www.cdc.noaa.gov/). Finally, we express our gratitude to one of the reviewers, who provided very useful and constructive comments for the manuscript.

Appendix A

Stochastic modelling of cyclone transits

The number of cyclone transits through any latitudinally oriented transect can be considered as a Poisson process. M06 demonstrated that a dispersion coefficient, $\hat{\psi}$, which identifies discrepancies between the winter mean $\bar{n}$ of monthly totals n_i of cyclone transits and the winter variance $s^2$of the monthly transit counts, can be used to interpret the time behaviour of the cyclones:

$$\hat{\psi} = \frac{s_{n^2}}{\bar{n}} - 1 \tag{A.1}$$

If,

$\hat{\psi} \approx 0$: This is consistent with a purely random process with constant rate.

$\hat{\psi} > 0$: Indication of overdispersion in the distribution of monthly transit counts. This case is consistent with a process that is more clustered in time than a purely random process.

$\hat{\psi} < 0$: Indication of underdispersion. This case is consistent with a process that is more regular than a purely random process with constant rate.

A method for estimating critical values for this dispersion statistic can be found in their appendix. These critical values are sample size dependent. For the observed 330 months of cyclone counts the null hypothesis of no under/overdispersion can be rejected at the 5% level for an estimated dispersion coefficient of approximately $\pm 12.8\%$. For the simulated 324 months the corresponding critical value is $\pm 12.9\%$.

Appendix B

Poisson regression

In the following, it is assumed that the monthly number N of cyclone transits through any latitude segment can be considered as an inhomogeneous one-dimensional Poisson process with time-varying rate. In this case we have that

$$N|\mu \sim \text{Poisson}(\mu).$$

This equation states that 'N given μ is Poisson distributed with mean μ'. Following M06, we employ a logarithmic link function to relate $\ln(\mu)$ to a linear combination of explanatory variables x_k.

$$\ln(\mu) = \beta_0 + \sum_{k=1}^{P} \beta_k x_k.$$

Maximum likelihood estimates of the regression parameters $\beta_k$can be obtained by means of an iterative weighted least squares algorithm. The x_k variables are five binary variables and ten teleconnection indices that together represent the mean state of the large scale flow for each month. The five binary variables are included in order to account for seasonality from October to March. Note that a sixth indicator variable is redundant since it is fully determined by the other five.

The indices of the ten leading teleconnections in the Northern Hemisphere were calculated based on the same method as the indices provided by the Climate Prediction Centre (www.cpc.noaa.gov/data/teledoc/telecontents.shtml). A rotational principal component analysis (RPCA) was applied to monthly mean standardized 500-mb height anomalies obtained from the NCEP in the region 20°N–90°N between January 1948 and October 2005. The resulting ten indices are by construction orthogonal and are therefore particularly useful as explanatory variables in the Poisson regression. The regression coefficients β_k are a measure of how the logarithm of the mean depends on the predictor variables x_k, for example a unit standard deviation change in the NAO.

References

Anderson, D., Hodges, K. I. and Hoskins, B. J. 2003. Sensitivity of feature-based analysis methods of storm tracks to the form of background field removal. *Mon. Wea. Rev.* **131**, 565–573.

Blackmon, M. L. 1976. A climatological spectral study of the 500-mb geopotential height of the Northern Hemisphere. *J. Atmos. Sci.* **33**, 1607–1623.

Bjerknes, V. 1910. Synoptical representation of atmospheric motions. *Quart. J. Roy. Meteor. Soc.* **36**, 167–286.

Bossouet, C., Deque, M. and Cariolle, D. 1998. Impact of a simple parameterization of convective gravity-wave drag in a stratosphere-troposphere general circulation model and its sensitivity to vertical resolution. *Ann. Geophys.-Atmos. Hydrospher. Space Sci.* **16**(2), 238–249.

Branstator, G. 1995. Organization of storm track anomalies by recurring low-frequency circulation anomalies. *J. Atmos. Sci.* **52**(2), 207–226.

Browning, K. A. 1990. Organization of clouds and precipitation in extratropical cyclones. *Extratropical Cyclones: The Erik H. Palmén Memorial Volume* (eds C. Newton and E. Holopainen), Amer. Meteor. Soc., 129–153.

Browning, K. A. 1999. Mesoscale aspects of extratropical cyclones: an observational perspective. *The Life Cycles of Extratropical Cyclones* (eds M. A. Shapiro and S. Grønås), Amer. Meteor. Soc., 265–283.

Browning, K. A., Hardman, M. E., Harrold, T. W. and Pardoe, C. W. 1973. Structure of rainbands within a mid-latitude depression. *Quart. J. Roy. Meteor. Soc.* **99**, 215–231.

Carlson, T. N. 1980. Airflow through midlatitude cyclones and the comma cloud pattern. *Mon. Wea. Rev.* **108**, 1498–1509.

Carlson, T. N. 1998. *Mid-Latitude Weather Systems*. Amer. Meteor. Soc., 507 pp.

Déqué, M., Dreveton, C., Braun, A. and Cariolle, D. 1994. The ARPEGE/IFS atmosphere model- a contribution to the French Community Climate Modeling. *Clim. Dyn.* **10**, 249–266.

Déqué, M., Marquet, P. and Jones, R. G. 1998. Simulation of climate change over Europe using a global variable resolution general circulation model. *Clim. Dyn.* **14**, 173–189.

Doblas-Reyes, F. J., Deque, M., Valero, F. and Stephenson, D. B. 1998. North Atlantic wintertime intraseasonal variability and its sensitivity to GCM horizontal resolution. *Tellus* **50A**, 573–595.

Douville, H., Royer, J. F. and Mahfouf, J. F. 1995. A new snow parameterization for the Meteo-France climate model. Part II: validation in a 3-D GCM experiment. *Clim. Dyn.* **12**(1), 37–52.

Eckhardt, S., Stohl, A., Wernli, H., James, P., Forster, C. and co-authors. 2004. A 15-year climatology of warm conveyor belts. *J. Clim.* **17**, 218–237.

Harrold, T. W. 1973. Mechanisms influencing the distribution of precipitation within baroclinic disturbances. *Quart. J. Roy. Meteor. Soc.* **99**, 232–251.

Hartmann, D. 1994. *Global Physical Climatology, Vol. 56, International Geophysics Series*, Academic Press, London.

Hodges, K. I. 1994. A general method for tracking analysis and its application to meteorological data. *Mon. Wea. Rev.* **122**, 2573–2586.

Hodges 1995. Feature tracking on the unit sphere. *Mon. Wea. Rev.* **123**, 3458–3465.

Hodges 1996. Spherical nonparametric estimators applied to the UGAMP model integration for AMIP. *Mon. Wea. Rev.* **124**, 2914–2932.

Hodges 1999. Adaptive constrains for feature tracking. *Mon. Wea. Rev.* **127**, 1362–1373.

Hodges, Hoskins, B. J., Boyle, J. and Thorncroft, C. 2003. A comparison of recent re-analysis datasets using objective feature tracking: storm tracks and tropical easterly waves. *Mon. Wea. Rev.* **131**, 2012–2037.

Hortal, M. 1998. Aspects of the numerics of the ECMWF model. *ECMWF Seminar Proceedings: Recent Developments in Numerical Methods for Atmospheric Modelling, 7 – 11 September 1998*, pp 127–143, ECMWF, Shinfield Park, Reading, Berkshire, UK.

Hoskins, B. J. 1983. Modelling of transient eddies and their feedback on the mean flow. *Large-Scale Dynamical Processes in the Atmosphere* (eds B. J. Hoskins and R. P. Pearce), Academic Press, 169–199.

Hoskins, B. J. and Hodges, K. I. 2002. New Perspectives on the Northern Hemisphere Winter Storm-Tracks*, J. Atmos. Sci.* **59**, 1041–1061.

Hoskins, B. J. and Valdes, P. J. 1990. On the Existence of Storm-Tracks. *J. Atmos. Sci.* **47**, 1854–1864.

Hurrell, J. W. 1995. Decadal trends in the North Atlantic Oscillation: regional temperatures and precipitation. *Science* **269**, 676–679.

Kalnay, E., Kanamitsu, M., Kistler, R., Collins, W., Deaven, D., and co-authors. 1996. The NCEP/NCAR 40-year reanalysis project. *Bull. Amer. Meteorol. Soc.* **77**, 437–471.

Kistler, R., Kalney, E., Collins, W., Saha, S., White, G., and co-authors. 2001. The NCEPNCAR 50-year reanalysis: monthly means CD-ROM and documentation. *Bull. Am. Meteorol. Soc.* **82,** 247–267.

Lau, N.-C. 1988. Variability of the observed midlatitude storm tracks in relation to low-frequency changes in the circulation pattern. *J. Atmos. Sci.* **45**, 2718–2743.

Lopez, P., Schmith, T. and Kaas, E. 2000. Sensitivity of the Northern Hemisphere circulation to North Atlantic SSTs in the ARPÈGE climate AGCM. *Clim. Dyn.* **16**, 535–547.

Lott, F. and Miller, M. J. 1997. A new subgrid-scale orographic drag parametrization: its formulation and testing. *Quart. J. Roy. Met. Soc.* **123 Part A**(537), 101–127.

Luksch, U., Raible, C. C., Blender, R. and Fraedrich, K. 2005. Decadal cyclone variability in the North Atlantic. *Meteorologische Zeitschrift* **14/6**, 747–753.

Mailier, P. J., Stephenson, D. B., Ferro, C. A. T. and Hodges, K. I. 2006. Serial clustering of extratropical cyclones, *Mon. Wea. Rev.* **134**, 2224–2240.

Morcrette, J.-J. 1991. Radiation and cloud radiative properties in the European Centre for Medium Range Forecasts forecasting sys-tem. *J. Geophys. Res.* **96**(D5), 9121–9132.

Peixoto, J. P. and Oort, A. H. 1992. *Physics of Climate*. American Institute of Physics, 520 pp.

Raible, C. C., Della-Marta, P., Schwierz, C., Wernli, H., Blender, R. 2008. Northern Hemisphere extratropical cyclones: a comparison of detection and tracking methods and different reanalyses. *Mon. Wea. Rev.,* in press.

Raible, C. C., Luksch, U., Fraedrich, K. and Voss, R. 2001. North Atlantic decadal regimes in a coupled GCM simulation, *Clim. Dyn.* **18**, 321–330.

Reynolds, R. W. and Smith, T. M. 1994. Improved global sea surface temperature analyses using optimum interpolation. *J. Clim.* **7**, 929–948.

Rogers, J. C. 1997. North Atlantic storm track variability and its association to the North Atlantic oscillation and climate variability of Northern Europe. *J. Clim.* **10**, 1635–1646.

Salari, I. and Sethi, K. 1990. Feature point correspondence in the presence of occlusion. *IEEE T. Pattern Anal.* **12**(1), 87–91

Simmons, A. J. and Burridge, D. M. 1981. An energy and angular momentum conserving vertical finite-difference scheme and hybrid vertical coordinate. *Mon. Wea. Rev.* **109**, 758–766.

Sorteberg, A., Kvamstø, N. G. and Byrkjedal, Ø. 2004. Wintertime Nordic Sea cyclone variability and its impact on oceanic volume transports into the Nordic Seas. *The Nordic Seas: An Integrated Perspective, Geophysical Monograph* **158**, 137–156.

Thompson, D. W. J. and Wallace, J. M. 1998. The Arctic Oscillation signature in the wintertime geopotential height and temperature fields. *Geophys. Res. Lett.* **25**, 1297–1300.

Zolina, O. and Gulev, S. K. 2002. Improving the accuracy of mapping cyclone numbers and frequencies. *Mon. Wea. Rev.* **130**, 748–759.